

A new quadrilateral 5-node non-conforming membrane element with drilling DOF

Tae-Yeol Lee[†] and Chang-Koon Choi[‡]

Department of Civil and Environmental Engineering,
Korea Advanced Institute of Science and Technology, Daejeon 305-701, Korea

(Received March 16, 2002, Accepted November 1, 2002)

Abstract. In this paper, a new quadrilateral 5-node non-conforming membrane element with drilling degrees of freedom is presented. The main advantage of these elements is the relatively small number of integration points to evaluate a stiffness matrix comparing to the existing transition membrane elements (CLM elements). Moreover, the presented elements pass the patch test by virtue of the Direct Modification Method incorporated into the element formulation. The presented 5-node elements are proved to be very efficient when used in the local mesh refinement for the in-plane structures which have stress concentrations. And some numerical studies also show the good performance of the new element developed in this study.

Key words: membrane element; drilling degrees of freedom; irregular node; midside node.

1. Introduction

Stress concentration occurs at the areas where abrupt geometrical changes exist, or at the points under concentrated loading. For such problems in many engineering practices, a finer mesh is used in the areas of high stress gradients while a rather coarser mesh is used where the stress distribution is relatively uniform.

One of the simplest ways to generate a locally refined finite element mesh in 2D problem is to connect the two layers of subdivided rectangular element to an undivided larger element by the use of hanging nodes (Bathe 1982, Hughes 1987). This approach requires additional treatment to preserve the compatibility between the refined and unrefined meshes, i.e., linear dependencies between the unknown nodal displacements should be established by means of application of constraints to the force-displacement equation. Zhu *et al.* (1991) suggested a meshing technique in which some distorted elements are used in the transition zone between the refined and coarse meshes. This approach does not require any constraints. However, it should be noted that the performance of the element is generally at its best when used without shape distortion.

Another possibility for mesh gradation as practiced by many investigators for the mesh transition is to use the triangular and quadrilateral elements together (Yunus *et al.* 1990, Evans *et al.* 1991).

[†] Postdoctoral Researcher

[‡] Institute Chair Professor

The constant strain triangular elements, however, show worse results in general than the quadrilaterals with the linear variation of strains and accordingly, the introduction of triangular elements to the mesh that consist mainly of quadrilateral elements can degrade the solution even if the quadrilaterals work well.

A successful way to generate a locally refined finite element mesh is to use the variable-node elements as transition elements (Choi and Park 1989, Choi and Park 1992, Choi and Lee 1995, Choi and Park 1997). Choi and Park (1992) effectively used the quadrilateral transition elements, which had a variable number of additional nodes on edges of a basic 4-node plate bending element to connect directly to the different layer patterns.

In Choi and Lee's study (1995), the Allman-type interpolation was successfully extended to develop the variable-node membrane elements with drilling degrees of freedom. In their study, 3×6 or 6×6 modified Gauss quadrature based on the sub-domain concept (Gupta 1978) was used to overcome the discontinuity of shape functions of the variable-node elements and 'B-bar' method (Wilson *et al.* 1990) are used to guarantee the element to pass the patch tests, which requires additional computing time to evaluate correction matrix. Consequently evaluation of the stiffness matrix requires more time and this can be regarded as the main shortcoming of these elements.

In this study, a new quadrilateral 5-node non-conforming membrane element with drilling degrees of freedom is presented. Quadratic shape functions, instead of the slope-discontinuous shape functions (Choi and Lee 1995), are adopted for variable mid-side nodes. By virtue of the continuous slope property of the quadratic shape functions, it is not required to use sub-domain concept for the element matrix computation any more. Thus, normal 3×3 Gauss integration or 8-point integration scheme can be used, that result in substantial reduction in computational time. Moreover, the Direct Modification Method (Choi *et al.* 2001), instead of 'B-bar' method, is successfully incorporated into the element formulation. Analyses for several numerical examples are carried out to demonstrate the validity and applicability of the present work.

2. Formulation of 5-node membrane element with drilling DOF

Fig. 1 shows the configuration of membrane elements which has an additional midside node. The interpolations for displacements and rotations are expressed by the same shape function N_i but the non-conforming modes \bar{N}_j are added to the displacements only. Fig. 2 shows the various non-conforming modes to be selectively used for the improvement of element behaviors.

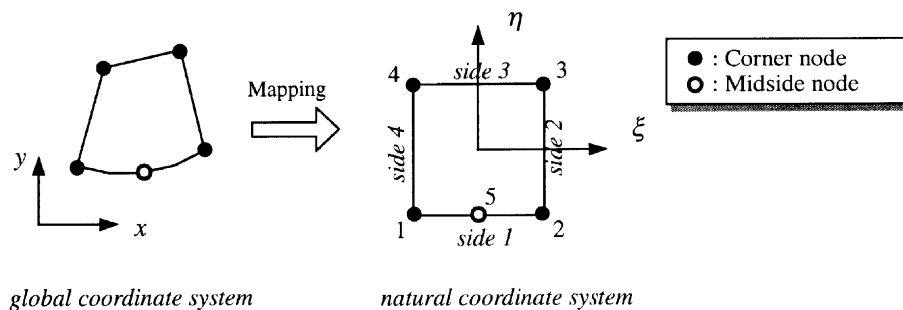


Fig. 1 Configuration of membrane elements with variable midside nodes

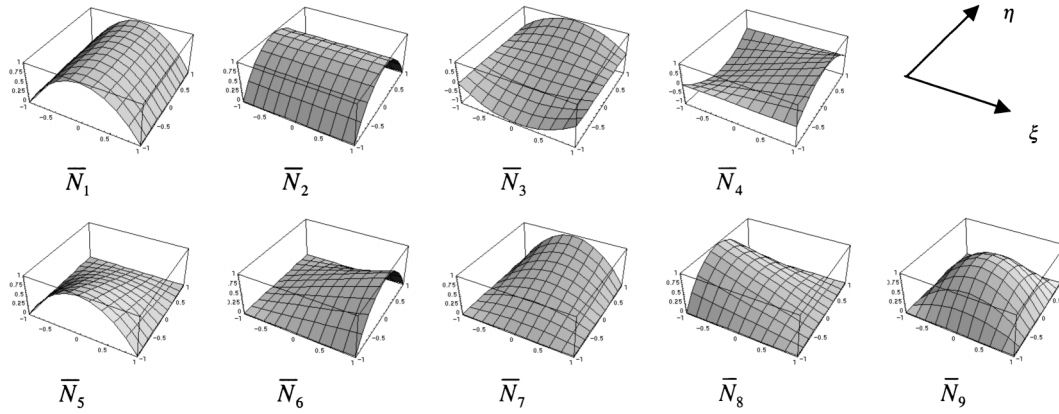


Fig. 2 Various non-conforming modes

$$N_i = \begin{bmatrix} N_i \\ N_i \end{bmatrix}, \quad \bar{N}_j = \begin{bmatrix} \bar{N}_j \\ \bar{N}_j \end{bmatrix} \tag{1}$$

where

$$\begin{aligned} N_1 &= N'_1 - \frac{1}{2}N_5 \\ N_2 &= N'_2 - \frac{1}{2}N_5 \\ N_3 &= N'_3 \\ N_4 &= N'_4 \end{aligned} \tag{2a}$$

$$\begin{aligned} N_5 &= \frac{1}{2}(1 - \xi^2)(1 - \eta) \\ N'_i &= \frac{1}{4}(1 + \xi_i \xi)(1 + \eta_i \eta), \text{ for } i=1, 2, 3, 4 \end{aligned} \tag{2b}$$

Fig. 3 shows the different locations of the fifth node of an element relative to the basic corner nodes. The stiffness matrices of the Type II~IV can be easily obtained by the transformation from that of Type I. Thus, only the formulation for Type I elements needs to be discussed in this paper.

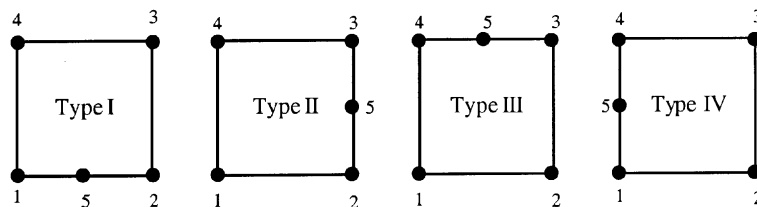


Fig. 3 Different type of 5-node element

To improve the basic behavior of original isoparametric type element, non-conforming displacement modes are added to the expression of original displacement field. Thus, the interpolated displacement and rotation fields for the membrane elements can be finally expressed as

$$\mathbf{u} = \begin{Bmatrix} u \\ v \end{Bmatrix} = \sum_{i=1}^5 N_i \mathbf{u}_i + \sum_{j=1}^m \bar{N}_j \bar{\mathbf{u}}_j \quad (3)$$

$$\boldsymbol{\theta} = \boldsymbol{\theta} = \sum_{i=1}^5 N_i \boldsymbol{\theta}_i \quad (4)$$

where m is the number of non-conforming modes used in the formulation.

The infinitesimal strains and rotations can be expressed using the differential operator as follows

$$\begin{aligned} \text{symm} \nabla \mathbf{u} &= \sum_{i=1}^5 \text{symm} \nabla N_i \mathbf{u}_i + \sum_j \text{symm} \nabla \bar{N}_j \bar{\mathbf{u}}_j \\ &= \sum_{i=1}^5 \mathbf{B}_i \mathbf{u}_i + \sum_j \bar{\mathbf{B}}_j \bar{\mathbf{u}}_j \\ &= [\mathbf{B} \quad \mathbf{0} \quad \bar{\mathbf{B}}] \begin{Bmatrix} \mathbf{u}^e \\ \boldsymbol{\theta}^e \\ \bar{\mathbf{u}}^e \end{Bmatrix} \end{aligned} \quad (5)$$

$$\begin{aligned} \boldsymbol{\theta} - \text{skew} \nabla \mathbf{u} &= \sum_{i=1}^5 N_i \boldsymbol{\theta}_i - \sum_{i=1}^5 \text{skew} \nabla N_i \mathbf{u}_i - \sum_j \text{skew} \nabla \bar{N}_j \bar{\mathbf{u}}_j \\ &= \sum_{i=1}^5 N_i \boldsymbol{\theta}_i + \sum_{i=1}^5 \mathbf{G}_i \mathbf{u}_i + \sum_j \bar{\mathbf{G}}_j \bar{\mathbf{u}}_j \\ &= [\mathbf{G} \quad \mathbf{N} \quad \bar{\mathbf{G}}] \begin{Bmatrix} \mathbf{u}^e \\ \boldsymbol{\theta}^e \\ \bar{\mathbf{u}}^e \end{Bmatrix} \end{aligned} \quad (6)$$

where \mathbf{B} and $\bar{\mathbf{B}}$ are the strain-displacement matrices of conforming and non-conforming part, respectively.

$$\mathbf{B} = \begin{bmatrix} N_{1,x} & 0 & N_{2,x} & 0 & N_{3,x} & 0 & N_{4,x} & 0 & N_{5,x} & 0 \\ 0 & N_{1,y} & 0 & N_{2,y} & 0 & N_{3,y} & 0 & N_{4,y} & 0 & N_{5,y} \\ N_{1,y} & N_{1,x} & N_{2,y} & N_{2,x} & N_{3,y} & N_{3,x} & N_{4,y} & N_{4,x} & N_{5,y} & N_{5,x} \end{bmatrix} \quad (7a)$$

$$\bar{\mathbf{B}} = \begin{bmatrix} \bar{N}_{1,x} & 0 & \bar{N}_{2,x} & 0 & \dots & \bar{N}_{m,x} & 0 \\ 0 & \bar{N}_{1,y} & 0 & \bar{N}_{2,y} & \dots & 0 & \bar{N}_{m,y} \\ \bar{N}_{1,y} & \bar{N}_{1,x} & \bar{N}_{2,y} & \bar{N}_{2,x} & \dots & \bar{N}_{m,y} & \bar{N}_{m,x} \end{bmatrix} \quad (7b)$$

\mathbf{G} , $\bar{\mathbf{G}}$, \mathbf{N} are vectors defined as follows;

$$\mathbf{G} = \langle -\frac{1}{2}N_{1,y} \quad \frac{1}{2}N_{1,x} \quad -\frac{1}{2}N_{2,y} \quad \frac{1}{2}N_{2,x} \quad -\frac{1}{2}N_{3,y} \quad \frac{1}{2}N_{3,x} \quad -\frac{1}{2}N_{4,y} \quad \frac{1}{2}N_{4,x} \quad -\frac{1}{2}N_{5,y} \quad \frac{1}{2}N_{5,x} \rangle \quad (8a)$$

$$\bar{\mathbf{G}} = \langle -\frac{1}{2}\bar{N}_{1,y} \quad \frac{1}{2}\bar{N}_{1,x} \quad -\frac{1}{2}\bar{N}_{2,y} \quad \frac{1}{2}\bar{N}_{2,x} \quad \dots \quad -\frac{1}{2}\bar{N}_{m,y} \quad \frac{1}{2}\bar{N}_{m,x} \rangle \quad (8b)$$

$$\mathbf{N} = \langle N_1 \quad N_2 \quad N_3 \quad N_4 \quad N_5 \rangle \quad (8c)$$

When $\bar{\mathbf{B}}$ and $\bar{\mathbf{G}}$ are used without any modification, the element cannot always pass the patch test due to the change in strain energy caused by addition of non-conforming modes (Choi *et al.* 2002). To solve this problem, Direct Modification Method (Choi *et al.* 2001) is adopted in this study and the modified matrices $\bar{\mathbf{B}}^*$ and $\bar{\mathbf{G}}^*$ are obtained as follows.

$$\bar{\mathbf{B}}^* = \begin{bmatrix} (\bar{N}_{1,x})^* & 0 & (\bar{N}_{2,x})^* & 0 & \dots & (\bar{N}_{m,x})^* & 0 \\ 0 & (\bar{N}_{1,y})^* & 0 & (\bar{N}_{2,y})^* & \dots & 0 & (\bar{N}_{m,y})^* \\ (\bar{N}_{1,y})^* & (\bar{N}_{1,x})^* & (\bar{N}_{2,y})^* & (\bar{N}_{2,x})^* & \dots & (\bar{N}_{m,y})^* & (\bar{N}_{m,x})^* \end{bmatrix} \quad (9a)$$

$$\bar{\mathbf{G}}^* = \langle -\frac{1}{2}(\bar{N}_{1,y})^* \quad \frac{1}{2}(\bar{N}_{1,x})^* \quad -\frac{1}{2}(\bar{N}_{2,y})^* \quad \frac{1}{2}(\bar{N}_{2,x})^* \quad \dots \quad -\frac{1}{2}(\bar{N}_{m,y})^* \quad \frac{1}{2}(\bar{N}_{m,x})^* \rangle \quad (9b)$$

Minimizing the functional, which takes into account the drilling degrees of freedom (Choi *et al.* 2002), for a single element, the expanded element stiffness matrix \mathbf{K}^e can be written as

$$\mathbf{K}^e = \begin{bmatrix} \mathbf{K}_{cc} & \mathbf{K}_{cn} \\ \mathbf{K}_{cn}^T & \mathbf{K}_{nn} \end{bmatrix} \quad (10)$$

where

$$\mathbf{K}_{cc} = \int_V \begin{bmatrix} \mathbf{B}^T \mathbf{D} \mathbf{B} & \mathbf{O} \\ \mathbf{O} & \mathbf{O} \end{bmatrix} dV + \alpha\mu \int_V \begin{bmatrix} \mathbf{G}^T \mathbf{G} & \mathbf{G}^T \mathbf{N} \\ \mathbf{N}^T \mathbf{G} & \mathbf{N}^T \mathbf{N} \end{bmatrix} dV \quad (11a)$$

$$\mathbf{K}_{cn} = \int_V \begin{bmatrix} \mathbf{B}^T \mathbf{D} \bar{\mathbf{B}}^* \\ \mathbf{O} \end{bmatrix} dV + \alpha\mu \int_V \begin{bmatrix} \mathbf{G}^T \bar{\mathbf{G}}^* \\ \mathbf{N}^T \bar{\mathbf{G}}^* \end{bmatrix} dV \quad (11b)$$

$$\mathbf{K}_{nn} = \int_V \bar{\mathbf{B}}^{*T} \mathbf{D} \bar{\mathbf{B}}^* dV + \alpha\mu \int_V \bar{\mathbf{G}}^{*T} \bar{\mathbf{G}}^* dV \quad (11c)$$

and \mathbf{D} is the constitutive matrix, and μ is the shear modulus. The problem dependent constant α is taken as 1.0 in this study. It is noted here that when $\alpha=0$ the second terms relating to the drilling degrees of freedom in Eqs. (11a-c) are zeros, the element stiffness matrix without drilling degrees of freedom is obtained.

The enlarged element stiffness matrix in Eq. (10) can be condensed back to the same size as the stiffness matrix of the ordinary membrane element by the static condensation.

$$\mathbf{K}^e = \mathbf{K}_{cc} - \mathbf{K}_{cn} \mathbf{K}_{nn}^{-1} \mathbf{K}_{cn}^T \quad (12)$$

3. Numerical integration

In general, the reduced integration techniques produce better overall results for the isoparametric type elements than the normal integration rules (Zienkiewicz *et al.* 1971). However, the uniformly reduced integration may produce the rank deficiency of stiffness matrix (Hughes 1987). Therefore, the modified integration rules need to be developed to avoid this type of problem. The 5-point rule and 8-point rule are successfully used in the numerical integration of various elements in the past (Stander and Wilson 1989, Groenwold and Stander 1995, Choi *et al.* 1999, Choi *et al.* 2002). Thus, it has been shown that the modified integration scheme improves the element behavior and at the same time, avoids the rank deficiency of uniformly reduced integration.

The first 5-node quadrilateral membrane element developed by Choi and Lee (1995) uses the slope-discontinuous shape functions, and thus requires the modified Gaussian quadrature based on sub-domain concept as shown in Fig. 4(a) (Gupta 1978). As the quadratic shape functions for mid-side node are used (see Eq. (2)) in this study instead of slope-discontinuous shape functions, the normal 3×3 Gaussian quadrature (Fig. 4(b)) or the 8-point integration scheme (see Fig. 4(c) and Table 1) can be selectively used.

Table 2 shows a series of NMD5-I to -VI elements systematically established according to the non-conforming modes added and the selective integration schemes used in the formulation, which can be regarded as a family of NMD4 elements developed recently (Choi *et al.* 2002). Here, NMD5-A stands for ‘5-node Non-conforming Membrane element with Drilling degrees of freedom-Type A’.

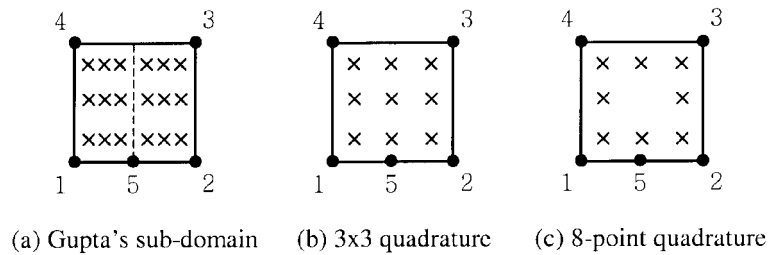


Fig. 4 Integration points of various integration scheme

Table 1 Modified reduced quadrature (8-point rule)

Point	Natural coordinates		Weight
	ξ_i	η_i	
1	-0.578803	-0.578803	0.99
2	0.578803	-0.578803	0.99
3	0.578803	0.578803	0.99
4	-0.578803	0.578803	0.99
5	0.000000	-0.578803	0.01
6	0.578803	0.000000	0.01
7	0.000000	0.578803	0.01
8	-0.578803	0.000000	0.01

Table 2 Types of membrane elements

Elements	Non-conforming modes	Integration schemes						Remark	
		K_{cc}		K_{cn}		K_{nn}			
		B^TDB	$\begin{matrix} G^TG \\ G^TN \\ N^TN \end{matrix}$	$\begin{matrix} B^TD\bar{B}^* \\ G^T\bar{G}^* \end{matrix}$	$N^T\bar{G}^*$	$\bar{B}^{*T}D\bar{B}^*$	$\bar{G}^{*T}\bar{G}^*$		
4-node	NMD4	$\bar{N}_1, \bar{N}_2, \bar{N}_3, \bar{N}_4$	2×2		2×2	3×3	5-point	2×2	Choi <i>et al.</i> (2002)
	NMD5-I	$\bar{N}_2, \bar{N}_4, \bar{N}_7, \bar{N}_9$	3×3			3×3		3×3	
	NMD5-II	$\bar{N}_2, \bar{N}_4, \bar{N}_7, \bar{N}_9$	3×3	2×2		2×2		2×2	
	NMD5-III	$\bar{N}_2, \bar{N}_4, \bar{N}_7, \bar{N}_9$	3×3	5-point		2×2		2×2	
5-node	NMD5-IV	$\bar{N}_2, \bar{N}_4, \bar{N}_7, \bar{N}_9$	3×3	5-point	8-point	3×3	8-point	3×3	This study
	NMD5-V	$\bar{N}_2, \bar{N}_4, \bar{N}_7$	3×3	5-point	8-point	3×3	8-point	3×3	
	NMD5-VI	$\bar{N}_2, \bar{N}_4, \bar{N}_7$	8-point	3×3	8-point	3×3	8-point	3×3	

4. Numerical analysis

4.1 Eigenvalue test

Eigenvalue analyses of a single unconstrained stiffness matrix have been performed in order to check the presence of spurious zero energy modes. All the elements presented in this study have correct numbers of zero eigenvalues associated with the rigid-body modes (Table 3) with an exception that the NMD5-II element has a rank deficiency.

The use of the element which possesses spurious zero energy modes should be avoided for practical engineering problems. Therefore, the element NMD5-II has been dropped out in the further consideration.

4.2 Patch test

In order to check if the presented 5-node membrane elements have the capability of representing constant strain states, the patch tests for two different layouts have been carried out (Fig. 5(a) and (b)).

Table 3 Eigenvalue test

Elements	Number of zero energy mode	Number of spurious zero energy mode
NMD5-I	3	0
NMD5-II	5	2
NMD5-III	3	0
NMD5-IV	3	0
NMD5-V	3	0
NMD5-VI	3	0

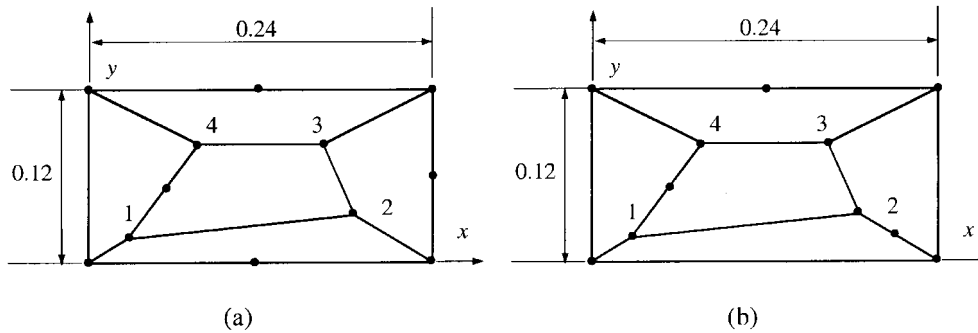


Fig. 5 Patch test

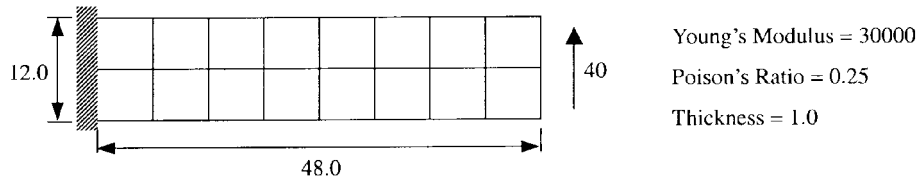
Table 4 Location of inner nodes

Node	x	y
1	0.04	0.02
2	0.18	0.03
3	0.16	0.08
4	0.08	0.08

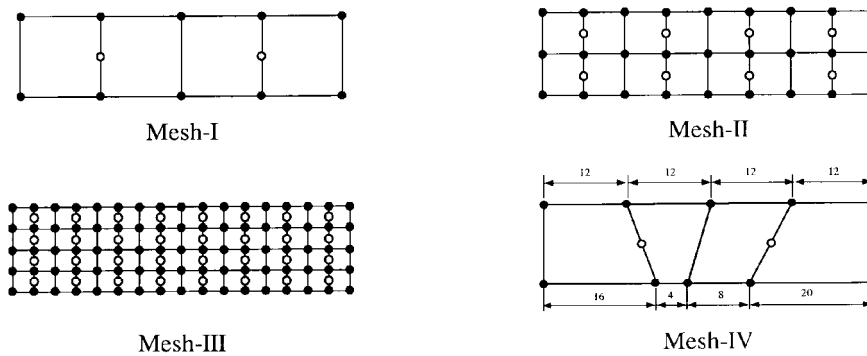
Each patch test model is composed by five elements with boundary conditions of $u = 10^{-3}(x + y/2)$, $v = 10^{-3}(y + x/2)$ as depicted in Fig. 5(a) and (b). The properties and dimensions used are given as Young's modulus $E = 1.0 \times 10^6$, Poisson's ratio $\mu = 0.25$, thickness $t = 0.001$, side length $a = 0.24$ and $b = 0.12$. Table 4 shows the locations of inner nodes in the patch and the mid-side nodes are located at the centers of element edges. All the presented elements produced the solutions which are exactly coincide with the theoretical solution of $\varepsilon_x = \varepsilon_y = \gamma = 10^{-3}$, $\sigma_x = \sigma_y = 1333$, $\tau_{xy} = 400$. These results show that the presented elements can give the stable convergence solution for locally refined mesh of the engineering problems which have stress concentration. The behavior of new element which has additional midside node added to the normal 4-node element is shown to be satisfactory.

4.3 A deep cantilever beam

A deep cantilever beam subjected to a parabolically distributed force along the free end side, as shown in Fig. 6(a), is a popular problem to examine the performance of element. The material properties are $E = 30000$, and $\mu = 0.25$. The elastic solution (Timoshenko and Goodier 1951) for the tip displacement is 0.3553 for the properties selected. The fixed boundary condition is idealized by constraining all the degrees of freedom. The results obtained are compared with 4-node NMD4 element and those from competing CLM (Choi-Lee Membrane) elements (Choi and Lee 1995). Good agreements are observed as listed in Table 5 in the case of regular mesh (Mesh-I-III). In the case of distorted mesh (Mesh-IV) the presented elements give as competitive tip displacements as CLM elements do in spite of the substantial reduction of integration points.



(a) Thick cantilever beam



- : Corner node
- : Midside node

(b) Mesh

Fig. 6 Thick cantilever beam

Table 5 The tip displacements of thick cantilever beam

Elements	Mesh				Remark	
	Mesh-I	Mesh-II	Mesh-III	Mesh-IV		
4-node	NMD4	0.3491	0.3517	0.3544	0.3298	Choi <i>et al.</i> (2002)
5-node	NMD5-I	0.3490	0.3543	0.3554	0.3200	This study
	NMD5-III	0.3491	0.3583	0.3582	0.3324	
	NMD5-IV	0.3480	0.3574	0.3567	0.3250	
	NMD5-V	0.3480	0.3573	0.3557	0.3220	
	NMD5-VI	0.3489	0.3616	0.3563	0.3240	
	CLM(Type-I)	0.3453	0.3519	0.3548	0.3148	Choi and Lee (1995)
CLM(Type-II)	0.3507	0.3536	0.3550	0.3236		
Reference value	0.3553					

4.4 Cook's problem

This problem was originally proposed by Cook as a test for the accuracy of quadrilateral elements (Fig. 7). Besides the shear dominant behavior, it also displays the effects of mesh distortion. The thickness of 1.0, Young's modulus 1.0 and Poisson's ratio of 1/3 were used, and applied load

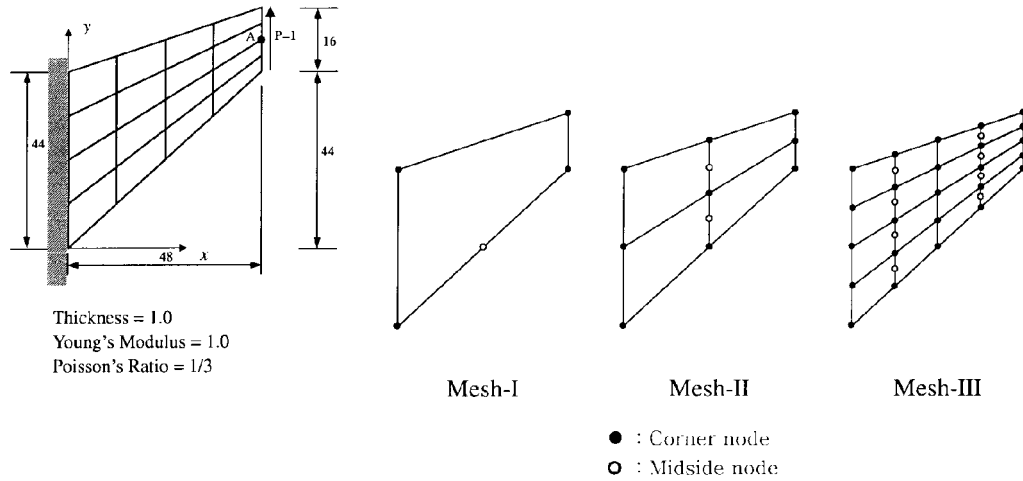


Fig. 7 Cook's membrane

Table 6 Tip displacements of Cook's problem

Elements	Tip displacements			Normalized value			Remark	
	Mesh-I	Mesh-II	Mesh-III	Mesh-I	Mesh-II	Mesh-III		
4-node	NMD4	16.72	22.97	23.67	0.699	0.961	0.990	Choi <i>et al.</i> (2002)
5-node	NMD5-I	20.26	20.61	23.03	0.847	0.862	0.963	This study
	NMD5-III	22.00	21.84	24.74	0.920	0.913	1.035	
	NMD5-IV	19.99	20.98	23.09	0.836	0.877	0.966	
	NMD5-V	19.66	20.56	23.11	0.822	0.860	0.967	
	NMD5-VI	20.47	21.07	23.18	0.856	0.881	0.969	
	CLM(Type-I)	18.71	19.67	22.86	0.783	0.823	0.956	
CLM(Type-II)	19.63	19.88	22.95	0.821	0.831	0.960		
Reference value		23.91			1.000			

$P = 1.0$ is distributed along edge side. The result for the tip deflection at point A is compared with the reference value 23.91 obtained by numerical analysis for a refined model (Bergan and Felippa 1985). Numerical tests with the sequentially refined meshes were carried out, and these test results are shown in Table 6 with those of other elements. It is noted that the presented elements give better results than CLM elements.

4.5 L-shaped panel under edge pressure load

To show the applicability of the presented element, the plane stress (or membrane) problems in an L-shaped panel under the edge pressure load are examined (Fig. 8). In this test, NMD5-VI elements presented in this study are used together with NMD4 elements (Choi *et al.* 2002). The properties and dimensions used are as follow: the elastic modulus $E = 100,000$ psi, Poisson's ratio $\nu = 0.3$,

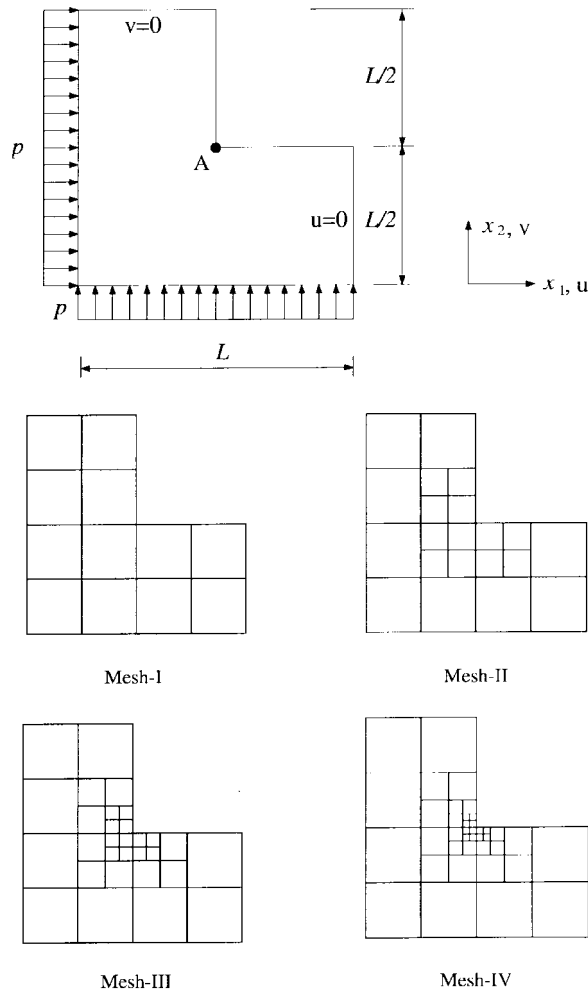


Fig. 8 L -shaped panel under edge pressure load

Table 7 Results of L -shaped panel

	Stress σ_{xy} at point A (psi)	NEL	TDOF	Remarks
Mesh-I	0.83	12	51	This study
Mesh-II	1.20	21	90	
Mesh-III	1.62	30	129	
Mesh-IV	2.18	39	168	
Reference value	2.22	768	2431	Choi <i>et al.</i> (2002)

NEL : Number of **E**lements

TDOF : Total number of **D**egrees **O**f **F**reedom

thickness $t = 1.0$ in, side length $L = 100.0$ in. and the edge pressure intensity of $p = 1.0$ lb/in.

Table 7 shows the obtained stress σ_{xy} at point A (Fig. 8) and the reference value was obtained

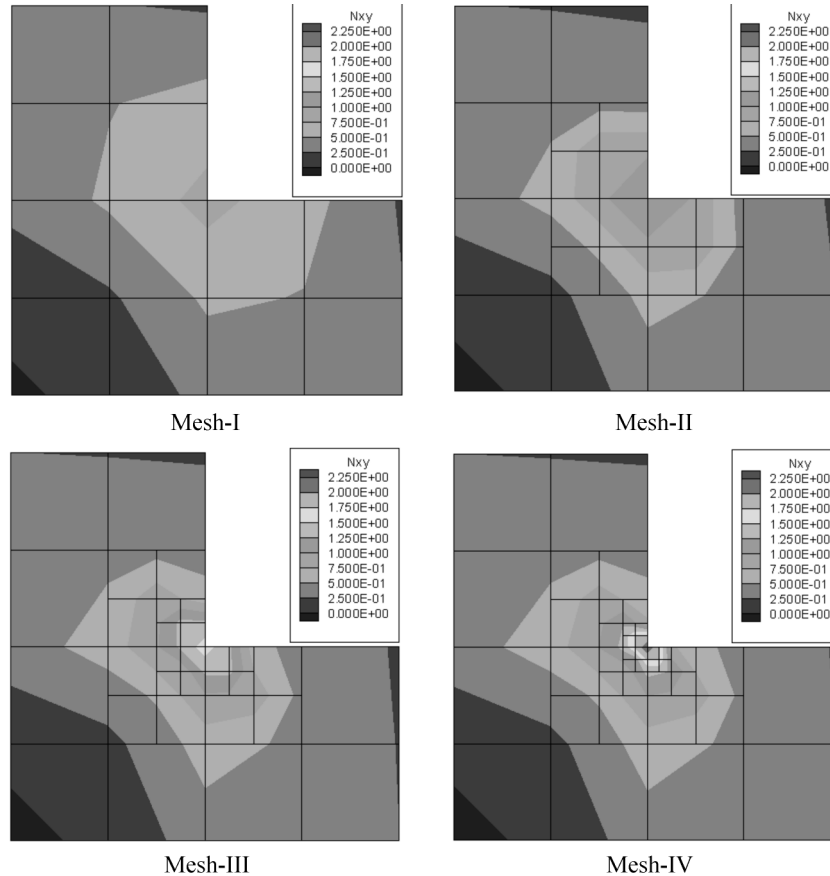


Fig. 9 Results of L -shaped panel under edge pressure load (stress contour : σ_{xy})

from very refined uniform mesh using NMD4 elements (Choi *et al.* 2002). The nodal stresses extrapolated from each Gauss points of the elements are averaged at each node and plotted in Fig. 9. The stress concentration near the point A, the number of elements (NEL), and total number of degrees of freedom (TDOF) used in the analyses are listed in Table 7 for comparison. The result from the Mesh-IV shows good agreement with that of very refined mesh even though relatively small number of TDOF was used. The validity and applicability of the presented elements in local mesh refinement is well demonstrated by this numerical example.

5. Conclusions

A series of 5-node non-conforming membrane elements with drilling degrees of freedom has been presented. The numerical test results show that the behavior of new element is very satisfactory. It passed the Eigenvalue test, Patch test and convergence test. The one of the advantages of these elements is that a smaller number of integration points are needed to evaluate a stiffness matrix of the element comparing to the existing transition membrane elements (CLM elements).

As shown in the results from the L -shaped panel under edge pressure load, the presented 5-node

elements can be effectively used for the practical engineering problems which have the high local stress concentration by generating locally refined mesh in an easy and effective manner. This characteristic is very important when the element is used for adaptive mesh refinement/recovery.

Behaviors of the elements in the series of new 5-node membrane quadrilaterals were very good. However, the best performance was obtained by the element NMD5-VI as shown in the test results in Tables 3,5,6. Therefore, the element NMD5-VI can be considered as the representative element of the entire elements in the series and designated simply as NMD5 in the practical applications.

These membrane elements can also be combined with a transition plate bending element to form a 5-node quadrilateral flat shell element which has 6 degrees of freedom at each node.

Acknowledgements

The authors would like to thank the Korea Science and Engineering Foundation (KOSEF) for their partial support of this work through Smart Infra structure Technology Center at Korea Advanced Institute of Science and Technology (KAIST).

References

- Bathe, K.J. (1982), *Finite Element Procedures in Engineering Analysis*, Prentice-Hall, New Jersey.
- Bergan, P.G. and Felippa, C.A. (1985), "A triangular membrane element with rotational degrees of freedom", *Comp. Meth. Appl. Mech. Eng.*, **50**, 25-69.
- Choi, C.K., Chung, K.Y. and Lee, T.Y. (2001), "A direct modification method for strains due to non-conforming modes", *Struct. Eng. Mech.*, **11**(3), 325-340.
- Choi, C.K., Lee, T.Y. and Chung, K.Y. (2002), "Direct modification for non-conforming elements with drilling DOF", *Int. J. Numer. Methods. Eng.*, **55**, 1463-1476.
- Choi, C.K. and Lee, W.H. (1995), "Transition membrane elements with drilling freedom for local mesh refinements", *Struct. Eng. Mech.*, **3**(1), 75-89.
- Choi, C.K. and Park, Y.M. (1989), "Nonconforming transition plate bending elements with variable midside nodes", *Comput. Struct.*, **32**, 295-304.
- Choi, C.K. and Park, Y.M. (1992), "Transition plate bending elements for compatible mesh gradation", *J. Eng. Mech. ASCE*, **118**(2), 462-480.
- Choi, C.K. and Park, Y.M. (1997), "Conforming and nonconforming transition plate bending elements for an adaptive *h*-refinement", *Thin Wall. Struct.*, **28**, 1-20.
- Evans, A., Marchant, M.J., Szmelter, J. and Weatherill, N.P. (1991), "Adaptivity for compressible flow computations using point embedding on 2-D structured multiblock meshes", *Int. J. Numer. Methods. Eng.*, **32**, 895-919.
- Groenwold, A.A. and Stander, N. (1995), "An efficient 4-node 24 d.o.f. thick shell finite element with 5-point quadrature", *Engineering Computations*, **12**, 723-747.
- Gupta, A.K. (1978), "A finite element for transition from a fine to a coarse grid", *Int. J. Numer. Methods. Eng.*, **12**, 35-45.
- Hughes, T.J.R. (1987), *The Finite Element Method-Linear static and dynamic finite element analysis*, Prentice-Hall, New Jersey.
- Hughes, J.R. and Brezzi, F. (1989), "On drilling degrees of freedom", *Comp. Methods Appl. Mech. Eng.*, **72**, 105-121.
- Stander, N. and Wilson, E.L. (1989), "A 4-node quadrilateral membrane element with in-plane vertex rotations and modified reduced quadrature", **6**, 266-271.
- Timoshenko, S. and Goodier, J.N. (1951), *Theory of Elasticity*, McGraw-Hill, New York.

- Wilson, E.L. and Ibrahimbegovic, A. (1990), "Use of incompatible displacement modes for the calculation of element stiffnesses or stresses", *Finite Elements in Analysis and Design*, **31**, 229-241.
- Yunus, S.M., Pawlak, T.P. and Wheeler, M.J. (1990), "Application of the Zienkiewicz-Zhu error estimator for plate and shell analysis", *Int. J. Numer. Methods. Eng.*, **29**, 1281-1298.
- Zhu, J.Z., Zienkiewicz, O.C. and Wu, J. (1991), "A new approach to the development of automatic quadrilateral mesh generation", *Int. J. Numer. Methods. Eng.*, **32**, 849-866.
- Zienkiewicz, O.C., Taylor, R.L. and Too, J.M. (1971), "Reduced integration technique in general analysis of plates and shells", *Int. J. Numer. Methods. Eng.*, **3**, 275-290.